IOP Conf. Series: Materials Science and Engineering **394** (2018) 032114 doi:10.1088/1757-899X/394/3/032114

Research on Machine Vision Inspection Technology of Tire Nail Hole

Menglong Cao, Libin Huo[a]

College of Automation and Electronic Engineering Qingdao University of Science and Technology Qingdao, China

[a]huolb22@163.com

Abstract. To solve the problem in the detection of tire nail holes which is caused by manual positioning or X-ray radiation, a machine vision technology-assisted high-voltage discharge detection system is designed to effectively detect the nail holes and accurately locate the holes. The Otsu is used to perform binarization of the image after the grayscale conversion. And the position of the nail hole is precisely positioned by tracking the object tracker of a specific color. After 5 groups of actual tests, we can accurately identify the location of the tire surface diameter of 2.5mm and above through holes, with the detection rate up to 92%.

1. Introduction

In the course of driving, the problem that tire is punctured by nails or hard objects often occurs which seriously affects driving safety and even endangers the lives of drivers. How to accurately and safely detect the location of nail holes has always been an important research point at home and abroad.

Research on the field of tire nail hole detection abroad has been carried out earlier. The vast majority of methods used in the study is using computer vision to detect the defects in the internal structure of the tire which is described by the structural texture features presented on the tire's X-ray image[1].This method requires high cost of equipment and produces X-rays that cause radiation to the human body.In reference [2], the non-destructive technique of acoustic emission (AE) method is proposed to detect defects, but it is only suitable for the smooth surface of the object. The concave and convex lines on the tire surface make this method not suitable for the detection of tire nail holes.

Compared with foreign detection technology research, domestic research on tire nail hole detection technology is still rare due to economic and technical factors. In domestic research methods, DSP (Digital signal processing) is used in [3]. In reference [4], an improved longitudinal dynamic threshold segmentation method based on the feature of tire X-ray image is adopted. Although the defect can be quickly detected by combining image processing in time domain and frequency domain, the radiation still exists. Reference [5] uses ultrasonic contrast test block method to detect defects, and [6] uses a SIFT feature descriptor matching algorithm based on sector region segmentation to identify feature points. However, different tire textures of different specifications can not be compared uniformly.

In view of the defects in the above methods, the tire nail hole detection system described herein uses a detection method combining the high-voltage discharge effect of minimum current with machine vision, so that the nail hole position can be identified more safely and accurately.

2. Overall Design of Tire Nail Hole Detection System

The principle of high voltage discharge of Tesla coil is that arc effect is produced to the opposite conductor by using high voltage and weak current which is harmless to human body. Machine vision can use the machine instead of human eyes to detect and judge. In this paper, a new method combining two techniques is adopted to ensure the safety of the tire nail hole detection system and to improve the recognition rate.

In this paper, the testing system of tire nail hole is operated by putting the tire on two rollers driven by step motor, which can be rotated synchronously, and the claw position can be adjusted by cylinder according to the actual size of the tire by clamping the tire wall with the claw of roller wheel.After the tire is fixed, a row of metal conductive curtains that connect to the positive electrode of the high pressure discharge system is attached to the inner wall of the tire, while the outer wall of the tire is attached to the cylinder of the negative electrode of the high pressure discharge system.As an insulator, if a pinhole appears when the tire rolls on the drum, the positive and negative electrode of the high voltage discharge system will form a path, which will produce arc discharge.At the same time, the machine vision system collects the image, that is, the camera located below the tire side transmits the captured image to the computer, and automatically recognizes the pinhole position by the grayscale transformation, the Otsu and the tracking and positioning method.The tire nail hole detection system mainly includes a high pressure system and a machine vision system, and the overall frame diagram is shown in FIG. 1 .

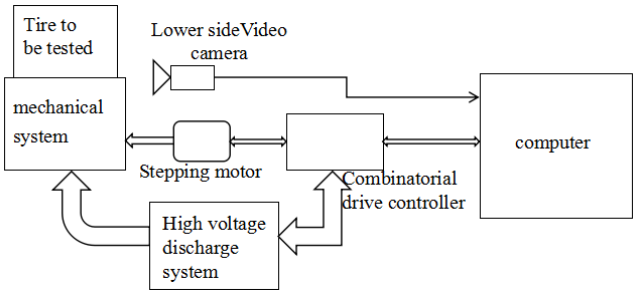

Fig.1. Frame chart of testing system for tire nail hole

3. Research on Algorithm of Machine Vision System

3.1. Grayscale Transformation

First, the acquired image is converted to a grayscale image. Grayscale images are obtained by measuring the brightness of each pixel in a single electromagnetic spectrum, such as visible light.The grayscale images used for display are usually stored on a nonlinear scale of 8 bits per sampled pixel, so that there can be 256 grayscales($2^8 = 256$). This precision has just been able to avoid visible band distortion and is very easy to program [7]. For an image, the corner points are related to the curvature characteristics of the autocorrelation function.The autocorrelation function describes the degree of change in the local image grayscale and can be expressed as:

$$E(x,y) = \sum_{u,v} \omega_{u,v} |I_{x+u,y+v} - I_{u,v}|^2 \quad (1)$$

In the equation, E(x, y) is the average change of image gray scale caused by the image window offset (x, y), ω is the image window, and I represents the image gray scale. At corners, the offset of the image window will cause a significant change in the autocorrelation function E(x, y) (the average change in image grayscale).

Formula (1) is developed at the pixel point (u, v). The autocorrelation function E(x, y) of the local image grayscale can be approximated as a Taylor polynomial:

$$E\ (x,y) = Ax^2 + By^2 + 2Cxy \tag{2}$$

In the equation, A, B, and C are approximations of second order differential, which can be expressed as:

$$A = X^2 \otimes h(x,y),\ B = Y^2 \otimes h(x,y),\ C = XY \otimes h(x,y)$$

$$X = I \otimes [1 \quad 0 \quad -1] \approx \frac{\partial I}{\partial x},\ Y = I \otimes [1 \quad 0 \quad -1]^T \approx \frac{\partial I}{\partial y}$$

In the equation, h(x, y) is a Gaussian smoothing filter function. X and Y are first-order directional differentials and can be represented by the image gray and x-direction difference operators [10, -1] and the y-direction difference operators [10, -1] T respectively.

In this way, (2) can be written as:

$$E\ (x,y) = [x \quad y] M \begin{bmatrix} x \\ y \end{bmatrix} \tag{3}$$

Here, the matrix M is the approximate Hessian matrix of the autocorrelation function E(x, y):

$$M(x,y) = \begin{bmatrix} A(x,y) & C(x,y) \\ C(x,y) & B(x,y) \end{bmatrix} \tag{4}$$

The extreme curvature of the autocorrelation function of image grayscale at a certain point can be approximately represented by the eigenvalue of the matrix. If the two eigenvalues of matrix M are large, it is shown that the extreme curvature of the two orthogonal directions of the autocorrelation function of image grayscale of this point is large, which can be considered as a corner point.

The determinant value of the matrix M (det [M]) is proportional to the product of the extreme curvature in two orthogonal directions. Therefore, the Haris corner detector is:

$$R(x,y) = \det[M(x,y)] - k \cdot trace^2[M(x,y)] \tag{5}$$

In the equation, det [M] =AB-C2 and trace [M] =A+B. As long as a certain point R(x, y) exceeds a certain threshold, the point is considered to be a corner point. According to Harris's suggestion, we can get better results when k is 0.04. In order to highlight the target or gray-scale interval of interest, that is, to emphasize the point of action of the highlight arc in this paper, and to relatively suppress those gray-scale regions that are not of interest, the piecewise linear method can be used. The gray scale mapping relationship of a pixel expressed by a calculation formula is:

$$g(i,j) = \begin{cases} \alpha f(i,j) & 0 \le f(i,j) < f_a \\ \beta(f(i,j) - f_a) + g(a) & f_a \le f(i,j) < f_b \\ \gamma(f(i,j) - f_b) + g(b) & f_b \le f(i,j) < 255_b \end{cases} \tag{6}$$

(i=1,2,...,m,j=1,2,...,n). In the equation, α, β, γ are the slopes of the three-segment broken line, so the collected image pixels are mapped into grayscale pixels. The transformed grayscale is compressed to reduce noise interference. The contrast map before and after gray scale transformation is shown in Figure 2:

(a) The image captured by a camera (b) Image after gray scale transformation

Fig 2. Contrast map before and after gray scale transformation

3.2. The Otsu image binarization

In order to further determine the position and boundary of nail holes, image binarization is used. A threshold T is set, above the threshold T is white, below the threshold T is black.The problem of identifying the nail hole position is then transformed into the problem of determining the threshold T. In many image binarization methods, the Otsu can effectively reduce the noise boundary and ensure the detection efficiency while improving the detection accuracy. It is divided into two parts: foreground and background according to the gray characteristic of the image. When the best threshold is taken, the difference between the two parts is the greatest. The standard used to measure the difference in the Otsu is the more common maximum variance between classes.The larger the class-to-background variance between the foreground and the background, the greater the difference between the two parts that make up the image, and when the segmentation of the threshold is taken to maximize the variance between classes, it means that the probability of misclassification is the smallest [8].

However, the Otsu is very sensitive to the noise and the target size (for example, due to uneven illumination, reflection, or complex backgrounds), and it is less effective for images with less difference between background and foreground. The CCD camera of the tire nail hole detection system is located below the side of the tire to be tested, and the external light is obscured by the tire, so the imaging brightness is less affected by the environment. After the grayscale transformation, the background of the bright arc and the almost black tire in the image is greatly different, effectively avoiding the defects of the Otsu. Therefore, this paper chooses the Otsu as the image binarization algorithm.

The T is the segmentation threshold of the foreground and background. The number of foreground spots accounts for ω_0, and the average grayscale is u_0.The number of background points in the image is ω_1 and the average grayscale is u_1. The total average grayscale of the image is u, and the variance of the foreground and background images is g. There are:

$$u = \omega_0 \times u_0 + \omega_1 \times u_1 \tag{7}$$

$$g = \omega_0 \times (u_0 - u)^2 + \omega_1 \times (u_1 - u)^2 \tag{8}$$

Simultaneously the above two formulas can be obtained:

$$g = \omega_0 \times \omega_1 \times (u_0 - u_1)^2 \tag{9}$$

Or

$$g = \frac{\omega_0}{1-\omega_0} \times (u_0 - u)^2 \tag{10}$$

When the variance g is the largest, it can be considered that the difference between the foreground and the background is the greatest. And the grayscale T at this time is the optimal threshold. In the Otsu, we exhaustively search for a threshold that minimizes the intra-class variance and is defined as the weighted sum of the variance of the two classes:

$$g_\omega(t) = \omega_2(t) g_2(t) + \omega_3(t) g_3(t) \tag{11}$$

The weights ω_2, ω_3 are the probabilities of the two classes separated by the threshold t, and gi is the variance of the two classes.

The Otsu also proves that minimizing intra-class variance and maximizing inter-class variance are the same:

$$g_b(t) = g - g_\omega(t) = w_1(t)\ w_2(t)[\mu_1(t) - \mu_2(t)]^2 \tag{12}$$

Wherein the class probability is represented by wi and the class mean is represented byμ_i.

$$w_1(t) = \sum_0^t p\ (i) \tag{13}$$

The class meanμ_1 (t) is:

$$\mu_1(t) = [\sum_0^t p\ (i)\ x\ (i)] / w_1 \tag{14}$$

Where X (i) is the value of the i-th bin center.

According to minimizing intra-class variance and maximizing inter-class variances and equal relationships, gray-scale images are automatically thresholded and verified by multiple groups of experiments. Finally, the Otsu threshold is automatically selected as 0.96, and the graythreshold is mapped to 246. This value can effectively overcome the effects of noise boundaries. That is, when t<246, the grayscale value of the pixel is f (t) =0; when t≥246, the grayscale value of the pixel is f (t) =255. The image comparison before and after binarization is shown in Figure 3:

(a)Image after gray scale transformation (b) binaryzation image

Fig 3. Image contrast before and after binarization

3.3. Nailing position tracking and positioning

After obtaining the binarized image, the position of the nail hole can be easily located by tracking the object tracker of the specific color [9]. The color information in the object tracker is sensitive to the lighting conditions, and the binarized image avoids the problem in a targeted manner, further eliminating noise interference. The pixels of the binarized image are brought to the HSV (Hue Saturation Value) space, then the tracker use the color space to track the given object according to the color and the threshold value, and the predefined color is white.

Using thresholds to process images, firstly, you need to use the HSV image to calculate the target area. Then, thresholds are used on the HSV spectrum to locate the desired "white" color and then the image is filtered based on the white color. Finally, use a rotating rectangle to draw an ellipse around the area of interest, which is the location of the nail hole. It is shown in Figure 4.

Fig 4. Location map of nail hole

4. Experimental Data Analysis

In order to test the effective diameter of the through hole that can be detected, using the method, five groups of man-made through-holes with diameters of 1mm, 1.5mm, 2mm, 2.5mm and 3mm were tested, and each group was tested 20 times. In this paper, no less than 80% is considered as the higher recognition rate, and the experimental results are shown in Table 1. The results show that when the diameter of the through hole is 1mm, it cannot be recognized. When the diameter is 1.5mm and 2mm, the recognition rate is low. And when the diameter is 2.5mm or more, the recognition rate is high. The actual measurement found that when the tire is pierced by a nail or other hard object to form a through hole, the diameter of the through hole is usually greater than 2.5mm, so the method will have a higher recognition rate for the naturally formed through hole.

Table 1. Different Nail Hole Diameter Recognition Result

Through hole size/(mm)	Recognition rate/%	Recognition rate assessment
1	0	Unrecognized
1.5	20	low
2	40	low
2.5	80	high
3	90	high

In order to verify the above conclusions and further compare the pinhole recognition rate of this method with that of the human eye method, the test subject was replaced with a through-hole formed naturally in daily use, and the diameter of the through hole was uncertain. After 5 groups of experiments, each group was tested 10 times to calculate the pin hole recognition rate. And Table 2 shows the comparison results that the method of this paper is 24% higher than the 68% recognition rate of human eyes, reaching 92%.

Table 2. Nail Holes Recognition Rate Comparison Result

experimental method	This article	Human eye
Group 1	90%	70%
Group 3	90%	70%
Group 3	90%	70%
Group 3	100%	60%
Group 3	90%	70%
average value	92%	68%

5. Conclusion

In this paper, the nail hole is found by high voltage discharge. And the ultra-low current is used at the same time, which is safer than the x ray detection method. Machine vision correlation algorithms are used to identify nail holes. First, grayscale conversion is used to convert the image to a grayscale image, highlighting the grayscale region of interest and reducing noise interference. Then, the threshold is automatically selected using the Otsu to binarize the image to overcome noise boundary affects. The progression of two algorithms, compared with other single algorithms, can reduce the noise twice, so that the noise can be ignored in the follow-up process. Finally, tracking the specific color "white" object tracker reduces the complexity of accurately locating the nail hole position.

The detection system of this paper has been verified by the nail hole recognition rate test, which can effectively detect the through hole of the tire with a diameter greater than or equal to 2.5mm, with the recognition rate of 92%. Compared with the human eye recognition rate, the recognition rate is significantly improved by 24%. How to further improve the detection rate of tire nail holes to achieve the goal of“zero missed inspection”is a direction that needs further improvement.

References

[1] WANG Yingmei, WANG Chuanxu. Tyre Defects Detection Based on Computer Vision. Information Technology and Informatization, 2013, vol. 6, pp. 101-103.
[2] Droubi M G, Faisal N H, Orr F, et al. Acoustic emission method for defect detection and identification in carbon steel welded joints. Journal of Constructional Steel Research, 2017, vol. 134, pp. 28-37.
[3] XIE Jun, HUANG Yi. Machine vision applications in the field of tire testing. Optical Instruments, 2013, vol. 3, pp. 32-35.
[4] ZHENG Xiaozhi. Tire Defect Detection Based on Integration Of Spatial and Frequency Domains. Shandong University of Finance and Economics, 2016.
[5] ZHANG Huan, Zhangxinju. Detection of Spring Surface Defects Based on Principle of Ultrasonic Surface Wave. Nondestructive Testing, 2015, vol. 6, pp. 43-45.
[6] ZENG Luan, GU Dalong. A SIFT Feature Descriptor Based on Sector Area Partitioning. Acta Automatica Sinica, 2012, vol. 9, pp. 1513-1519.
[7] Dou Y, Zheng Y Q. Research on Boundary Detection for Turnout Rail Components Based on Machine Vision. Applied Mechanics & Materials, 2013, pp. 303-306, pp. 617-620.
[8] ZHANG Guimei, ZHANG Song, CHU Jun. A New Object Detection Algorithm Using Local Contour Features. Acta Automatica Sinica, 2014, vol. 10, pp. 2346-2355.
[9] Prince S J D. Computer Vision: Models, Learning, and Inference. Cambridge University Press, 2012